American Journal of Signal Processing 2020, 10(1): 1-9
DOI: 10.5923/j.ajsp.20201001.01

An Exact Pseudo-Static Time-Domain Theory of Natural Pulse Width Modulation

Dante C. Youla[1], Fred Winter[2,*]

[1]New York University Tandon School of Engineering, United States
[2]Advanced Energy, United States

Abstract Owing in part to the increasing importance of pulse width modulation (PWM) as an alternative analog communication technique for optical data links there has been a resurgence of interest in both new and traditional methods of analysis. Of the latter, the old pseudo-static approach is undoubtedly the simplest, although long considered by many to be only an approximation. One principal object of this paper is to prove that pseudo-static analysis is exact and explicit for natural ramp-intersective PWM and allows easy derivation of all pertinent time-domain formulas. As shown in detail by example, it then may be possible to carry out spectral and modulation-demodulation analysis in a straightforward physically insightful quantitative manner.

Keywords Ramp Intersective, PWM, Modulation, Demodulation, Spectral Analysis, Pseudo Static, Exact

1. Introduction

The problem of determining the properties of a periodic square-wave of period T which has been pulse width modulated (PWM) by a bounded deterministic signal *x(t)* is an old one dating back to World War II [1]. In a paper published in 2003 [2], Z. Song and D.V. Sarwarte not only review some of the relevant literature, but also find explicit formulas for the expansions in terms of *x(t)* of both uniform and natural PWM[1]. Their analysis of the latter presents the greatest difficulty and is accomplished with the aid of a theorem of Lagrange in the theory of complex variables [3]. It appears, however, that use of this theorem is only justified when *x(t)* admits an analytic continuation into the complex t-plane, a superfluous technical constraint owed to the approach, rather than any fundamental limitation.

Our main purpose is to demonstrate that all such extraneous requirements can be eliminated with the help of a key observation whose generality seems to have been overlooked in previous studies. Namely, that the classical intuitive pseudo-static analysis of natural PWM [1], by far one of the most commonly employed, *is exact instead of just an approximation!* It employs two mild assumptions which are easily imposed in practice:

$$\text{A}_1.\ \underbrace{sup}_{t}\ |x(t)| < 1; \tag{1a}$$

$$\text{A}_2.\ |x(t_2) - x(t_1)| \leq \mu\ |t_2 - t_1|, \tag{1b}$$

μ a real positive constant and (t_1, t_2) any real pair.

Although the Lipschitz condition (1b) implies the continuity of *x(t)*, it does not imply either its boundedness or differentiability. Nevertheless, if the first derivative *x'(t)* of *x(t)* exists and is uniformly bounded, i.e., if

$$c \triangleq \underbrace{sup}_{t}\ |x'(t)| < \infty, \tag{1c}$$

it then follows (from Rolle's theorem) that (1b) holds with the choice $\mu = c$.

2. The Pseudo – Static View of Natural PWM

Implementation of natural PWM by the ramp-intersective method is depicted in detail in Figure 1(a). The modulation is either single-edge (SE) or double-edge (DE), depending on whether one or both edges of the pulse are allowed to shift in time. Moreover, SE decomposes into exclusively trailing-edge (TE) or exclusively leading-edge (LE).

As seen from Fig. 1(b), the TE pulse train $p_m(t; x; TE)$ is generated by comparing *x(t)* to the ramp *r(t)* of slope *2/T* in every interval *(kT, (k+1)T)*. The comparator returns the value 1 if the difference *x(t)-r(t)* is positive and the value 0 if not. Similarly, the LE pulse train $p_m(t; x; LE)$ in Fig. 1(c) is obtained by comparing *x(t)* to the ramp of slope *-2/T*. Lastly, the DE pulse train $p_m(t; x; DE)$ in Fig. 1(d). utilizes the two

* Corresponding author:
fred.winter@aei.com (Fred Winter)
Published online at http://journal.sapub.org/ajsp

[1] Natural PWM is accomplished by means of the ramp-intersective method described in section 2.

dashed-line ramps $r_N(t)$ and $r_P(t)$ of slopes $-4/T$ and $4/T$ to fix the location and width d_k-c_k of the corresponding pulse. Quantitatively, the comparator reads 1 iff $x(t)-r_N(t)$ and $x(t)-r_P(t)$ are both positive and reads 0, otherwise.

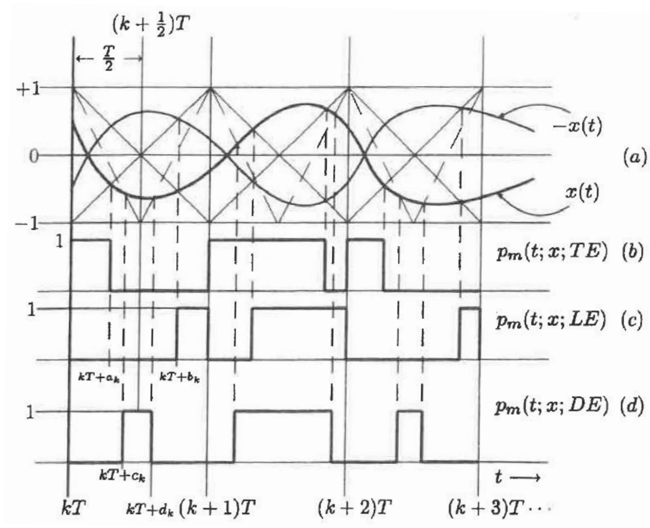

Figure 1. The Generation of Natural TE, LE and DE by ramp-intersection

Four facts of interest emerge that are worth singling out:

1. Periodicity of the ramps does not imply that of any of the three pulse trains;
2. For the TE case the leading edge is fixed at kT and the trailing edge can move, for the LE case the trailing edge is fixed at $(k+1)T$ and the leading edge can move, while in the DE case both edges can move and no symmetry about the $(k+1/2)T$ line need exist;
3. Each of the three pulse trains contributes only one pulse to every time slot

$$\mathbb{I}_k(T) \triangleq (kT < t < (k+1)T);$$

4. Examination of Fig. 1(a) reveals that the ramp of slope $2/T$ intersects $-x(t)$ at the same instant that the ramp of slope $-2/T$ intersects $x(t)$. From this equality one easily infers the 1's complement identity

$$p_m(t;\,-x;\,TE) + p_m(t;\,x;\,LE) = 1, \tag{2}$$

a useful algebraic result[2].

Any one of the pulse trains, be it TE, LE or DE, may be viewed as a pulse-coded version of an information bearing signal x(t) and knowledge of their spectral content can be essential. The pseudo-static approach to deriving this content begins by considering the TE, LE and DE trains as created in two separate steps.

In the first, the trailing edge, leading edge and the two edges of 50% duty cycle periodic waveforms $p(t)$, $p(t-T/2)$ and $p(t-T/4)$ of period T are shifted statically by the respective amounts $\tau T/2$, $\tau T/2$ and $\tau T/4$ in the directions indicated in Fig. 2. At this stage τ is considered to be a constant parameter subject to the sole inequality

$$-1 < \tau < 1. \tag{3}$$

Pulse widening occurs if $\tau > 0$, narrowing if $\tau < 0$ and the numerical changes in width are less than $T/2$.

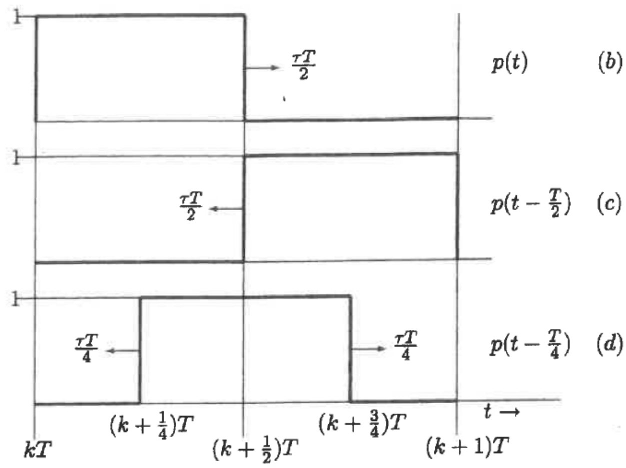

Figure 2

Denote the periodic extensions of period T of these three modified pulses by $\mathbb{I}_{TE}(t;\,\tau)$, $\mathbb{I}_{LE}(t;\,\tau)$ and $\mathbb{I}_{DE}(t;\,\tau)$. Each possesses a Fourier series expansion in t whose coefficients depend on the parameter τ. Substitution of $x(t)$ for τ defines corresponding functions of time $\mathbb{I}_{TE}(t;\,x(t))$, $\mathbb{I}_{LE}(t;\,x(t))$ and $\mathbb{I}_{DE}(t;\,x(t))$. In the second step it is accepted, often on physical grounds, that the *"approximations"*

$$I_{TE}(t;\,x(t)) \sim p_m(t;\,x;\,TE), \tag{4}$$

$$I_{LE}(t;\,x(t)) \sim p_m(t;\,x;\,LE) \tag{5}$$

and

$$I_{DE}(t;\,x(t)) \sim p_m(t;\,x;\,DE) \tag{6}$$

are sufficiently accurate to be of engineering significance. It perhaps is unexpected to discover that this conjecture is more than right on the mark.

The Pseudo-Static (PS) Theorem: Let $x(t)$ satisfy assumptions A_1 and A_2. Then

$$I_{TE}(t;\,x(t)) = p_m(t;\,x;\,TE), \tag{7}$$

$$I_{LE}(t;\,x(t)) = p_m(t;\,x;\,LE) \tag{8}$$

and

$$I_{DE}(t;\,x(t)) = p_m(t;\,x;\,DE). \tag{9}$$

As an excellent illustration of the power of this theorem we shall use it to routinely derive series expansions for TE, LE, and DE natural PWM.

In the interval $(0,\,T)$,

$$I_{TE}(t;\,\tau) = \begin{cases} 1, 0 < t < \frac{T(1+\tau)}{2}, \\ 0, otherwise. \end{cases} \tag{10}$$

Hence the coefficients C_r in its complex Fourier series are given by

$$c_o = \frac{1+\tau}{2} \tag{11}$$

[2] 1), 2), and 4) require little explanation and 3) holds whenever $1/T > \mu/2$ (Proof postponed).

and

$$c_r = \frac{1}{T}\int_0^{\frac{T(1+\tau)}{2}} e^{-jr\omega_c t}dt = \frac{1-e^{-jr\omega_c\frac{T(1+\tau)}{2}}}{2\pi jr} \quad (12)$$

$$= \frac{1-e^{-jr\pi(1+\tau)}}{2\pi jr} = \frac{1-(-1)^r e^{-jr\pi\tau}}{2\pi jr}, \quad (13)$$

where, $r = \pm 1, \pm 2, \cdots$, and $\omega_c = 2\pi/T$. Consequently (easy details omitted),

$$I_{TE}(t;\ \tau) = \frac{1+\tau}{2} + \sum_{r=1}^{\infty}\frac{\sin r\omega_c t}{r\pi} + \sum_{r=1}^{\infty}(-1)^{r-1}\frac{\sin r(\omega_c t-\pi\tau)}{r\pi}. \quad (14)$$

It then follows from (7) and (2) that

$$p_m(t;\ x;\ TE) = \frac{1+x(t)}{2} + \sum_{r=1}^{\infty}\frac{\sin r\omega_c t}{r\pi} + \sum_{r=1}^{\infty}(-1)^{r-1}\frac{\sin r(\omega_c t-\pi x(t))}{r\pi} \quad (15)$$

and

$$p_m(t;\ x;\ LE) = \frac{1+x(t)}{2} - \sum_{r=1}^{\infty}\frac{\sin r\omega_c t}{r\pi} - \sum_{r=1}^{\infty}(-1)^{r-1}\frac{\sin r(\omega_c t+\pi x(t))}{r\pi}. \quad (16)$$

As regards the DE pulse train, observe that in *(0,T)*

$$I_{DE}(t;\tau) = \begin{cases} 1, \frac{T(1-\tau)}{4} < t < \frac{T(3+\tau)}{4}, \\ 0, otherwise. \end{cases} \quad (17)$$

Therefore $c_o = (1+\tau)/2$ and

$$c_r = \frac{1}{T}\int_{\frac{T(1-\tau)}{4}}^{\frac{T(3+\tau)}{4}} e^{-jr\omega_c t}dt = \frac{-e^{-jr\frac{\pi(1-\tau)}{2}} - e^{-jr\frac{\pi(3+\tau)}{2}}}{2\pi jr}, \quad (18)$$

where, $r = \pm 1, \pm 2, \cdots$,. Accordingly, (some details omitted)[3],

$$I_{DE}(t;\ \tau) = \frac{1+\tau}{2} + \sum_{r=1}^{\infty}(-1)^r\frac{\sin r(\omega_c t+\frac{\pi(1+\tau)}{2}) - \sin\ r(\omega_c t-\frac{\pi(1+\tau)}{2})}{r\pi} \quad (19)$$

$$= \frac{1+\tau}{2} + 2\sum_{r=1}^{\infty}(-1)^r\frac{\sin(\frac{r\pi(1+\tau)}{2})}{r\pi}\cos r\omega_c t, \quad (20)$$

so that

$$p_m(t;\ x;\ DE) = \frac{1+x(t)}{2} + 2\sum_{r=1}^{\infty}(-1)^r\frac{\sin(\frac{r\pi(1+x(t))}{2})}{r\pi}\cos r\omega_c t. \quad (21)$$

Unlike TE and LE, in DEPWM all carrier harmonics are suppressed, a possible advantage for some telecommunication applications [4].

Instead of *p(t)*, *p(t-T/2)* and *p(t-T/4)*, Song and Sarwarte choose to work with the unmodulated carriers

$$q(t) = 2p(t) - 1 = \begin{cases} 1, 0 < t < \frac{T}{2}, \\ -1, \frac{T}{2} < t < T, \end{cases} \quad (22)$$

q(t-T/2), and *q(t-T/4)*. Concomitantly,

$$q_m(t;x;TE) = 2p_m(t;x;TE) - 1, \quad (23)$$

$$q_m(t;x;LE) = 2p_m(t;x;LE) - 1 \quad (24)$$

and

$$q_m(t;x;DE) = 2p_m(t;x;DE) - 1. \quad (25)$$

A quick check confirms that

$$q_m(t;\ x;\ TE) = x(t) + 2\left(\sum_{r=1}^{\infty}\frac{\sin r\omega_c t}{r\pi} + \sum_{r=1}^{\infty}(-1)^{r-1}\frac{\sin r(\omega_c t-\pi x(t))}{r\pi}\right), \quad (26)$$

$$q_m(t;\ x;\ LE) = x(t) - 2\left(\sum_{r=1}^{\infty}\frac{\sin r\omega_c t}{r\pi} + \sum_{r=1}^{\infty}(-1)^{r-1}\frac{\sin r(\omega_c t+\pi x(t))}{r\pi}\right) \quad (27)$$

and

$$q_m(t;\ x;\ DE) = x(t) + 4\sum_{r=1}^{\infty}(-1)^r\frac{\sin(\frac{r\pi(1+x(t))}{2})}{r\pi}\cos r\omega_c t \quad (28)$$

agree with Equations (37), (44) and (63) in [2].

3. Solution of a Classical Problem

The availability of time-domain expansions for the various pulse trains almost invariably simplifies the derivation of their spectral properties.

Example: Determine the spectrum of the TE pulse-train *pm(t; x; TE)* in (15) under single-tone modulation $x(t) = E_m \sin\omega_m t$, $0 < E_m < 1$.

Solution: It is first necessary to find the frequency content of the second sum $S_2(t)$ in (15). Evidently[4],

$$S_2(t) = \sum_{r=1}^{\infty}\frac{(-1)^r}{r\pi}\sin r(\pi E_m \sin\omega_m t - \omega_c t) \quad (29)$$

$$= \sum_{r=1}^{\infty}\frac{(-1)^r}{r\pi}\, Im(e^{-jr\omega_c t}e^{jr\pi E_m \sin\omega_m t}) \quad (30)$$

$$= \sum_{r=1}^{\infty}\frac{(-1)^r}{r\pi}\, Im(e^{-jr\omega_c t}\sum_{n=-\infty}^{\infty}J_n(r\pi E_m)\, e^{jn\omega_m t}) \quad (31)$$

$$= \sum_{r=1}^{\infty}\frac{(-1)^{r-1}}{r\pi}\sum_{n=-\infty}^{\infty}J_n(r\pi E_m)\sin(r\omega_c - n\omega_m)t \quad (32)$$

$$= -\sum_{r=1}^{\infty}\frac{1}{r\pi}\sum_{n=-\infty}^{\infty}J_n(r\pi E_m)\sin((r\omega_c - n\omega_m)t - r\pi). \quad (33)$$

By extracting the *n = 0* component of (32) and adding it to the sum

$$S_1(t) = \sum_{r=1}^{\infty}\frac{\sin r\omega_c t}{r\pi} \quad (34)$$

In (15) we obtain the complete decomposition

$$p_m(t;\ x;\ TE) = \frac{1+E_m \sin\omega_m t}{2} + \sum_{r=1}^{\infty}\frac{1+(-1)^{r-1}J_0(r\pi E_m)}{r\pi}\sin r\omega_c t - R(t), \quad (35)$$

where

$$\mathrm{R(t)} = \sum_{r=1}^{\infty}\sum_{n=1}^{\infty}J_n(r\pi E_m)\frac{1}{r\pi}\{\sin((r\omega_c - n\omega_m)t - r\pi) + (-1)^n\sin((r\omega_c + n\omega_m)t - r\pi)\}. \quad (36)$$

The original proof of this result by WR Bennett in 1933 was accomplished with the aid of a double Fourier series technique [7,8].

[3] $\sin\alpha - \sin\beta = 2\cos\frac{\alpha+\beta}{2}\sin\frac{\alpha-\beta}{2}$.

[4] $J_n(z)$ is the Bessel function of the first kind of order n and argument z [3]
$J_{-n}(z) = (-1)^n J_n(z)$, $e^{ja\sin\theta} = \sum_{n=-\infty}^{\infty}J_n(a)e^{jn\theta}$
and Im[z] is the imaginary part of the complex number z.

4. Proof of the PS Theorem

Consider justification of equation (9) and recall that $I_{DE}(t;\ \tau)$ represents the periodic extension of the modified pulse shown in Fig. 2(d), obtained by shifting the leading and trailing edges of $p(t-T/4)$ to the left and right, respectively, by the same amount $\tau T/4$. The resultant modified pulse has width $T(1+\tau)/2$. Write

$$I_{DE}(t;\tau) = \sum_{r=-\infty}^{\infty} c_r(\tau) e^{jr\omega_c t}. \quad (37)$$

What must be established is that

$$I_{DE}(t;x(t)) \triangleq \sum_{r=-\infty}^{\infty} c_r(x(t)) e^{jr\omega_c t} = p_m(t;\ x;\ DE)\ . \quad (38)$$

Let $kT < t_0 < (k+1)T$, t_0 fixed, but arbitrary, and note that

$$I_{DE}(t_0;x(t_0)) = \sum_{r=-\infty}^{\infty} c_r(x(t_0)) e^{jr\omega_c t_0} \quad (39)$$

Is the value of

$$f(t) \triangleq \sum_{r=-\infty}^{\infty} c_r(x(t_0)) e^{jr\omega_c t} \quad (40)$$

for $t = t_0$. Since $f(t)$ is a period T periodic function, its structure is known. Indeed, in $I_k(T) \triangleq (kT < t < (k+1)T)$, $f(t)$ is a unit-magnitude rectangular pulse with leading and trailing edges located at the respective translates

$$\frac{T}{4}(1-x(t_0)) + kT \text{ and } \frac{T}{4}(3+x(t_0)) + kT \quad (41)$$

of the points $T(1 - x(t_0))/4$ and $T(3 + x(t_0))/4$ on the t-axis of $I_0(T) = (0 < t < T)$. Accordingly, $f(t_0) = 1$, iff

$$\frac{T}{4}(1-x(t_0)) + kT < t_0 < \frac{T}{4}(3+x(t_0)) + kT \quad (42)$$

and equals 0 otherwise. Equivalently, such is true iff

$$x(t_0) > \frac{4}{T}(t_0 - kT) - 3 \text{ and } x(t_0) > 1 - \frac{4}{T}(t_0 - kT). \quad (43)$$

Or, expressed more compactly, iff $x(t_0) > r_p(t_0)$ and $x(t_0) > r_N(t_0)$, where

$$r_p(t) = \frac{4}{T}(t - kT) - 3 \text{ and } r_N(t) = 1 - \frac{4}{T}(t - kT) \quad (44)$$

are the equations in $I_k(T)$ of the positive and negative slope dashed-line ramps shown in Fig. 1(a). To sum up, for t in $I_k(T)$, $I_{DE}(t;\ x(t)) = 1$ iff $x(t)$ is greater than both $r_p(t)$ and $r_N(t)$ and is 0 if not, precisely the rule prescribed in section 2 for the ramp-intersective formation of the pulse train $p_m(t;\ x;\ DE)$ in Fig. 1(d). The proofs of (7) and (8) proceed along very similar lines[5]. Hence, guided by footnote 5 we obtain, without difficulty,

$$x(t) > \begin{cases} r(t) \rightarrow I_{TE}(t;\ x(t)) = 1, \\ -r(t) \rightarrow I_{LE}(t;\ x(t)) = 1, \end{cases} \quad (45)$$

where

$$r(t) = \frac{2(t-kT)}{T} - 1 \quad (46)$$

is the equation in $I_k(T)$ of the positive-slope solid-line ramp shown in Fig. 1(a). Moreover, if > in (45) is changed to <, *1* is changed to *0, Q.E.D.*

[5] For example, in $I_k(T)$ the function $f(t) = I_{LE}(t;\ x(t_0))$ is a unit-magnitude rectangular pulse with leading and trailing edges located at $T(1-x(t_0))/2+kT$ and $(k+1)T$, respectively. Hence $f(t_0)=1$ iff $t_0 > T(1-x(t_0))/2+kT$, i.e., if f $x(t_o) > 1-(t_0-kt)2/T = -r(t_0)$, etc..

5. Overview

The pulse trains in Figs. 1(a), (b), and (c) are monopulse, in the sense that each contributes only a single pulse to every interval $I_k(T)$. This need not be true in general, but is always achievable by making T sufficiently small, i.e., by choosing the sampling rate $1/T$ large enough. For the proof, assume that $x(t)$ makes contact with the ramp $r(t)$ in (46) at distinct points t_1, t_2, in $I_k(T)$. Then $x(t_1) = r(t_1)$, $x(t_2) = r(t_2)$ and

$$\frac{1}{T} = \frac{x(t_2)-x(t_1)}{2(t_2-t_1)} \quad (47)$$

follows. Consequently, in view of assumption A_2,

$$\frac{1}{T} \leq \frac{|x(t_2)-x(t_1)|}{2|t_2-t_1|} \leq \frac{\mu}{2}. \quad (48)$$

Clearly, when $1/T > \mu/2$, (48) is contradictory and distinct multiple ramp contacts are precluded.[6] But a pulse train generated without multiple ramp contacts is necessarily mono.

If the convergence of the several infinite series is accepted [7], it appears that our proof of the PS theorem is of a truly elementary character. It relies almost entirely on the realization that the value of $I_{DE}(t;\ x(t))$ for any given $t=t_0$ equals the value of $f(t) = I_{DE}(t;\ x(t_0))$ for $t=t_0$. Since $f(t)$ is of period T and of known rectangular shape fully defined by $p(t)$ and $x(t_0)$, this value is immediately determined.

Also, as a matter of practical concern, it is useful to know that bandlimited functions $x(t)$ of finite energy are automatically bounded and always satisfy assumption A_2 [9]. In this case it is possible to enforce A_1 by ordinary amplitude scaling.

6. Demodulation of Single-Tone Modulated TE, LE and DE Pulse Trains

The Bennett decomposition of the TE pulse train $p_m(t;\ x;\ TE)$ generated by single-tone modulation $x(t) = E_m \sin \omega_m t$ is displayed in equations (35) and (36). Close examination under the assumption $\omega_c / \omega_m > 1$ reveals that ideal low-pass filtering of radian bandwidth ω_m will, when applied to $p_m(t;\ x;\ TE)$ as input, produce an output which in addition to the information bearing waveform $(1+x(t))/2$, contains other terms that account for distortion and are contributed by the double sum

$$\sum_{r=1}^{\infty} \sum_{n=1}^{\infty} (-1)^{r+1} J_n(r\pi E_m) \frac{\sin(r\omega_c - n\omega_m)t}{r\pi}. \quad (49)$$

Introduce the positive parameter $k \triangleq \omega_c / \omega_m$. Then k is > 1 and

$$\sin(r\omega_c - n\omega_m)t = \sin(rk-n)\omega_m t\,. \quad (50)$$

Consequently, a component (50) in (49) lies in the passband of the filter (and therefore adds to the distortion), iff $|rk - n| \leq 1$ or, iff the integers r and n obey the

[6] Naturally, $1/T > \mu/2 \Rightarrow 1/T > \mu/4$ and distinct multiple contacts with the ramps $r_p(t)$ and $r_N(t)$ in (44) are similarly ruled out.

inequality

$$-1 \le n - rk \le 1; \tag{51}$$

i.e., iff

$$rk - 1 \le n \le rk + 1. \tag{52}$$

Let $[rk]$ and $\langle rk \rangle$ denote, respectively, the largest integer $\le rk$ and the smallest integer $\ge rk$. From (52)[7]

$$\langle rk \rangle - 1 \le n \le [rk] + 1. \tag{53}$$

Evidently, if rk is an integer, $\langle rk \rangle = [rk] = rk$ and the allowed values of *n* are given by

$$n = rk - 1, rk, rk + 1. \tag{54}$$

But if rk is not an integer, $\langle rk \rangle = [rk] + 1$ and now only pairs

$$n = [rk], [rk] + 1 \tag{55}$$

are permitted. Correspondingly, if $k > 1$ is prescribed in advance and $D_r(k)$ denotes the distortion produced by term r in (49), then for rk an integer,

$$D_r(k) = \frac{(-1)^{r+1}}{r\pi}\left(J_{rk-1}(r\pi E_m) - J_{rk+1}(r\pi E_m)\right) \sin \omega_m t. \tag{56}$$

When, however, rk is not an integer, it may be rewritten as $k = [rk] + \epsilon_r$, where $0 < \epsilon_r < 1$, so that

$$D_r(k) = \frac{(-1)^{r+1}}{r\pi}\{ J_{[rk]}(r\pi E_m) \sin \epsilon_r \omega_m t \\ -J_{[rk]+1}(r\pi E_m) \sin(1-\epsilon_r)\omega_m t \} \tag{57}$$

is a weighted sum of two complementary subharmonics of $\sin \omega_m t$.[8] Of course, as is obvious, k an integer implies all rk integers, whereas k not an integer implies that some rk, $r \ge 2$ are not integers. In the first case the total distortion is of the form $C(k) \sin \omega_m t$, where $C(k)$ is the sum over $r = 1 \to \infty$ of the coefficients of $\sin \omega_m t$ in (56), while in the second the sum of the $D_r(k)$ in (57) always includes subharmonics. In fact, with irrational k all distortion is subharmonic.[9]

It should now be apparent that the normalized quantity

$$\eta(k) \triangleq \frac{C(k)}{E_m} = \sum_{r=1}^{\infty} (-1)^{r+1} \frac{J_{rk-1}(r\pi E_m) - J_{rk+1}(r\pi E_m)}{r\pi E_m} \tag{58}$$

is an appropriate measure of total distortion when k is an integer greater than one.[10] Some simplification is possible, for replacement of l by rk and z by $r\pi E_m$ in the Bessel function identity [11]

$$2 J_l'(z) = J_{l-1}(z) - J_{l+1}(z) \tag{59}$$

transforms (58) into

$$\frac{1}{2}\beta\eta(k) = \sum_{r=1}^{\infty} (-1)^{r-1} \frac{J_{rk}'(r\beta)}{r}, \tag{60}$$

a series of the *Kaptyen* type [11], in which the modulation index $\beta = \pi E_m$ is $< \pi$ because the modulation depth E_m satisfies $0 < E_m < 1$. Let $\epsilon = \beta/k$ and suppose that $0 < \epsilon \le 1$. For fixed k and β, $J_{rk}'(r\beta)$ is positive and decreases monotonically as $r \to \infty$.[11]

Proof. According to Watson [11, Pgs. 253,254] for $\nu > 0$ and $0 < \epsilon \le 1$, both $J_\nu(\nu\epsilon)$ and $J_\nu'(\nu\epsilon)$, when viewed as functions of ν with ϵ held fast, are positive and decrease monotonically as ν increases. To make use of the second of these two properties, write

$$J_{rk}'(r\beta) = J_{rk}'(rk\epsilon) \tag{61}$$

and observe that an increase of r to $r+1$ may be interpreted as an increase of ν from rk to $(r+1)k$ in the function $J_\nu'(\nu\epsilon)$, without change in $\epsilon = \beta/k$, Q.E.D.

Corollary (important): For, $0 < \epsilon \le 1$ the quantities $\frac{J_{rk}'(r\beta)}{r}$ in (60) are positive and decrease, monotonically, to zero as $r \to \infty$. Thus (60) is an alternating series that meets the *Leibnitz null-monotone* requirement. It therefore converges [12] and the remainder R_l after l terms is always numerically less than the numerical value of the first term neglected, i.e.,

$$| R_l | < \frac{J_{rk}'(r\beta)}{r} |_{r=l+1}. \tag{62}$$

It seems evident from symmetry considerations that equation (60) for $\eta(k)$ should also be valid for single-tone modulated LE pulse trains. A more informative analytic proof, however, is had by referring back to (35) and (36) to conclude with the help of the 1's complement identity (2), that all LE distortion is contributed by the terms in the sine-wave summation[12]

$$\sum_{r=1}^{\infty} \sum_{n=1}^{\infty} (-1)^{r+n} \frac{J_n(r\beta) \sin(rk-n)\,\omega_m t}{r\pi E_m} \tag{63}$$

that get passed by the low-pass filter. Accordingly, addition of the particular terms corresponding to $n = rk - 1$ and $= rk + 1$, etc. leads to (58) and then quickly to (60), provided k is an *even* positive integer.[13] Of course $k > 1$ and $0 < \epsilon = \beta/k \le 1$ are again necessary constraints.

To demonstrate the applicability of (60) to single-tone modulated DE pulse trains, we set $x(t) = E_m \sin \omega_m t$ in (21) and then perform spectral analysis in the manner used to derive the Bennett partition in equations (35), (36). As a first step we ask the reader to verify that the second term in (21) may be rewritten in the expanded form

$$\sum_{r=1}^{\infty} \frac{(-1)^r}{r\pi} \sum_{n=-\infty}^{\infty} J_n(r\frac{\beta}{2})\{ \sin(\frac{r\pi}{2} + (\mathrm{rk}+\mathrm{n})\,\omega_m t) + \\ \sin(r\pi 2 - (rk - n)\omega m t) \}. \tag{64}$$

With the aid of the identity $J_{-n}(z) = (-1)^n J_n(z)$, we readily see[14] that the only sine waves that can contribute to distortion are those of radian frequencies $\le \omega_m$ contained

---

[7] $k - 1 \le n \Rightarrow rk \le 1 + n \Rightarrow \langle rk \rangle \le 1 + n$, and $n \le rk + 1 \Rightarrow n - 1 \le rk \Rightarrow n - 1 \le [rk]$.

[8] Specifically, $\epsilon_r\,\omega_m + (1-\epsilon_r)\,\omega_m = \omega_m$.

[9] These subharmonics are often partly responsible for unacceptable pulse-train jitter at the receiving end of a fiber-optic data link [10]

[10] With this notation the filter output may be expressed as

$$y(t) = \frac{1 + x(t)}{2} + x(t)\eta(k). \tag{59a}$$

Clearly, the use of the estimator

$$2y(t) - 1 = x(t) + 2x(t)\eta(k) \tag{59b}$$

for $x(t)$ entails a 200 $\eta(k)$ percent error in the estimate of either $x(t) = E_m \sin \omega_m t$ *or* E_m.

[11] $J_{rk}'(r\beta) \triangleq \frac{dJ_{rk}(z)}{dz}|_{z=r\beta}$

[12] $-x(t) = -E_m \sin \omega_m t = E_m \sin(-\omega_m)t$.

[13] $(-1)^{r+n} = (-1)^{r+rk-1} = (-1)^{r+rk+1} = (-1)^{r-1}$ when the integer k is even because $(-1)^{rk} = 1$ and $(-1)^{r+1} = (-1)^{r-1}$.

[14] The n = 0 term lies outside the filter bandwidth and may be ignored.

in the sum

$$S(n) = \sum_{r=1}^{\infty}\frac{1}{r\pi}\sum_{n=1}^{\infty}J_n(r\tfrac{\beta}{2})\{ (-1)^r \sin(\tfrac{r\pi}{2}-(rk-n)\,\omega_m\, t) + (-1)^{r+n}\sin(\tfrac{r\pi}{2}+(rk-n)\omega_m\, t)\Big\} \qquad (65)$$

Assume, once again, that k is an even integer > 1 and let us compute $S(n)$ for the three permitted values $= rk-1, rk, rk+1$:

$$S(rk-1) = 2(\ \sum_{r=1}^{\infty}(-1)^{r-1}\cos\frac{r\pi}{2}\ \frac{J_{rk-1}\left(\frac{r\beta}{2}\right)}{r\pi}\ )\sin\omega_m t\ ; \qquad (66)$$

$$S(rk) = 2(\ \sum_{r=1}^{\infty}(-1)^{r}\sin\frac{r\pi}{2}\ \frac{J_{rk}\left(\frac{r\beta}{2}\right)}{r\pi}\ ) \qquad (67)$$

and

$$S(rk+1) = -2(\ \sum_{r=1}^{\infty}(-1)^{r-1}\cos\frac{r\pi}{2}\ \frac{J_{rk+1}\left(\frac{r\beta}{2}\right)}{r\pi}\ )\sin\omega_m t\ . \qquad (68)$$

Since $S(rk)$ is an irrelevant and removable DC pedestal, the sum of the coefficients of $\sin\omega_m t$ in (66) and (68), divided by E_m, is the obviously correct measure of total normalized distortion $\eta(k)$.

Hence

$$\frac{1}{4}\beta\eta(k) = \sum_{r=1}^{\infty}(-1)^{r-1}\cos\frac{r\pi}{2}\ \frac{J'_{rk}\left(\frac{r\beta}{2}\right)}{r}. \qquad (69)$$

But cos(rπ/2) = 0 for r odd and equals $(-1)^l$ for r = $2l$ even. Concomitantly,

$$\frac{1}{2}\beta\eta(k) = \sum_{l=1}^{\infty}(-1)^{l-1}\frac{J'_{2lk}(l\beta)}{l}. \qquad (70)$$

This is an alternating series of the *Leibnitz null-monotone* type when k, in addition to being an even integer > 1, also meets the requirement $0 < \beta/2k \le 1$.[15]

Demodulation Theorem: The total distortion $\eta(k)$ incurred by using ideal low-pass filtering to demodulate the three pulse trains created by natural single-tone pulse-width modulation is determined from equations (60) and (70). Specifically, assume k to be an integer > 1. Then

1. for *TE* use (60) $with\ 0 < \beta/k \le 1$;
2. for *LE* use (60) $with\ k\ even\ and\ 0 < \beta/k \le 1$;
3. for *DE* use (70) $with\ k\ even\ and\ 0 < \beta/2k \le 1$.

7. Numerical Results for the Design Engineer

Problem Statement for the Engineer

The problem statement of interest to the design engineer begins with reference to footnote 10, equation (59b), of this paper. There, $\eta(k)$ is seen to quantify the level of distortion to be tolerated in the process of demodulation of x(t). Equation (60) shows that $\eta(k)$ is calculated from a series whose terms are composed of Bessel function derivatives. Furthermore, (60) also reveals that $\eta(k)$ is a function of k and β. So, the task for the engineer is to determine the smallest k for a given β and a given upper bound on $|\eta(k)|$. Equation (60) applies in the cases of TE and LE PWM, while (70) applies to the case of DE PWM. Initially, the discussion will center on (60) with the understanding that (70) is understood similarly and is appropriately clarified in the sequel.

Computation of Bessel Function Series Coefficients

Numerical tabulation of the series coefficients makes use of (59) combined with the Bessel function tables found in [13]. The coefficient data is tabulated and appears in Tab.'s 1(a) and 2(a). We will need to use this data both to estimate $\eta(k)$ and to estimate the percent error associated with our estimate of $\eta(k)$. Theoretical underpinnings are developed next to make effective use of this numerical data to solve the design problem as stated.

Theoretical Underpinnings for Numerical Procedures

Absent a closed form solution for the value of $\eta(k)$ in (60), one may then proceed to numerically estimate $\eta(k)$. We are fortunate that this series is a member of the class of alternating series known as the Leibnitz null-monotone class. This is the best of all series with many desirable properties, convergence among them, that permit numerical estimation of $\eta(k)$. We begin by writing $\eta(k)$ as follows. Let

$$\eta(k) = S_l(k) + R_l(k), \qquad (71)$$

where $S_l(k)$ represents a finite sum obtained by taking the first l terms in (60) and the infinite series $R_l(k)$ is the remainder. We will represent the approximation of $\eta(k)$ by $S_l(k)$ as

$$\eta(k) \sim S_l(k), \qquad (72)$$

when l is to be large enough to result in a satisfactory estimate. The formal solution to this estimation problem [15] can be stated as

$$|\,\eta(k) - S_l(k)| \le r_{l+1} \qquad (73)$$

where, r_{l+1} is used designate the real number which is the absolute value of the first term of $R_l(k)$ in (71).

While (73) provides an answer to the number of decimal places of agreement one can expect in (72), an additional figure of merit which permits us to estimate the "percent error" associated with our estimate of $\eta(k)$ is useful. This "percent error" is designated as $\delta\eta_l(k)$ and is formulated[16] as

$$\delta\eta_l(k) = \frac{R_l(k)}{S_l(k)+R_l(k)}. \qquad (74)$$

An admissible[17] $\eta(k)$ as well as it's associated $S_l(k)$ *'s* must converge to a nonzero[17] value. Rewriting (74) by dividing by $S_l(k)$ is then well-defined for any l, infinity included. If we also make use of the triangle inequality we

[15] $J'_{2lk}(l\beta) = J'_{2lk}(2lk\frac{\beta}{2k})$ *is an instance of* $J'_\nu(\nu\epsilon)$ *with* $\nu = 2lk$ *and* $= \frac{\beta}{2k}$, *etc.*

[16] The actual percent error is of course obtained after multiplication of $\delta\eta_l(k)$ obtained in (74) by 100.

[17] We of course assume that $S_1(k)$ *and* $S_2(k)$ for the alternating series are each nonzero and of like sign. A series constrained in this manner necessarily converges to a finite nonzero sum. If such were not true in PWM, say, there would be no distortion error to consider in x(t) to begin with.

can write an upper bound for $\delta\eta_l(k)$ as

$$|\delta\eta_l(k)| \le |\frac{R_l(k)}{S_l(k)}| \frac{1}{1-|\frac{R_l(k)}{S_l(k)}|}. \tag{75}$$

The properties of alternating series alone [15] permit us to bound $R_l(k)$ in (75) by r_{l+1} and write

$$|R_l(k)| \le |r_{l+1}|. \tag{76}$$

Combining (75) with (76) we recognize that in place of a specific series like (60), we have focused our considerations on the properties of an entire admissible class of alternating series. We have then proven the following

Theorem: The percent error $\delta\eta_l(k)$ is bounded by (77) when partial sums $S_l(k)$ of an admissible alternating series $\eta(k)$ are employed in its approximation. Thus,

$$|\delta\eta_l(k)| \le |\frac{r_{l+1}}{S_l(k)}| \frac{1}{1-|\frac{r_{l+1}}{S_l(k)}|}. \tag{77}$$

Table 1(a). Bessel Function Derivative Coefficients

	β k	1 3	1 4	2 4	1 5	2 5	3 5
series term *r*	k, β relation β/k	k=β+2 1/3	k=β+3 1/4	k=β+2 1/2	k=β+4 1/5	k=β+3 2/5	k=β+2 3/5
1	$\frac{J'_{rk}(r\beta)}{r}$	0.05621150	0.00965510	0.06093000	0.00122803	0.01348000	0.06030500
2		0.00171628	0.00004310	0.00356035	0.00000062	0.00022550	0.00478050
3		0.00008008	0.00000029	0.00031922	0.0000000005	0.00000476	0.00058362
4		0.00000445	0.000000002	0.00003415		0.00000012	0.00008508
5		0.00000027		0.00000402		0.000000003	0.00001367
6		0.00000002		0.00000050			0.00000233
7				0.00000007			0.00000042
8				0.00000001			0.00000008

Table 1(b). Estimation of η by S_l using coefficients from Table 1(a)

k	β	*l*	*1*	*2*	*3*	*4*	*5*	*6*	*7*
4	1	S_l	0.01931020	0.01922400	0.01922459				
	2		0.06093000	0.05736965	0.05768887	0.05765472	0.05765874	0.05765824	0.05765831
4	1	error bound on $\lvert\eta - S_l\rvert$	0.00008620	0.00000059	0.000000005				
	2		0.00356035	0.00031922	0.00003415	0.00000402	0.00000050	0.00000007	0.00000001
4	1	error bound on $\delta\eta_l$	0.00448419	0.00003065	0.00000025				
	2		0.06205982	0.00559534	0.00059228	0.00006980	0.00000874	0.00000114	0.00000015
4	1	error bound on $\lvert S_l - S_{l+1}\rvert$ *l odd*	0.00008620						
	2		0.00008620		0.00003415		0.00000050		

Table 2(a). Bessel Function Derivative Coefficients

	β k	1 6	2 6	3 6	2 7	3 7	3 8
series term *r*	k, β relation β/k	k=β+5 1/6	k=β+4 2/6	k=β+3 3/6	k=β+5 2/7	k=β+4 3/7	k=β+5 3/8
1	$\frac{J'_{rk}(r\beta)}{r}$	0.00012415	0.00343255	0.02022800	0.00058991	0.00544830	0.00123130
2		0.00000001	0.00000758	0.00047883	0.00000024	0.00003163	0.00000149
3			0.00000004	0.00001742	0.0000000002	0.00000028	0.000000003
4				0.00000076		0.000000003	
5				0.00000004			

Table 2(b). Estimation of η by S_l using coefficients from Table 1(a)

k	β	*l*	*1*	*2*	*3*	*4*
7	2	S_l	0.00058991	0.000589668	0.000589669	
	3		0.00363220	0.00361112	0.0036113033	0.0036113013
7	2	error bound on $\lvert\eta - S_l\rvert$	0.00000024	0.0000000002		
	3		0.00002108	0.00000019	0.000000002	
7	2	error bound on $\delta\eta_l$	0.00040973	0.00000026		
	3		0.00583882	0.00005206	0.00000055	
7	2	error bound on $\lvert S_l - S_{l+1}\rvert$ *l odd*	0.00000024			
	3		0.00002108		0.0000000020	

Observing the null-monotone property of such series, we are permitted to state that[18]

$$|R_l\,(k)| \;\le |S_l(k)|, any\ l. \tag{78}$$

This result calls attention to the fact that as l increases the quantity in (79) holds for any admissible $\eta(k)$, namely,

$$\left|\frac{R_l\,(k)}{S_l(k)}\right| \le 1, any\ l. \tag{79}$$

As l increases the left side of (79) becomes ever smaller[18] than the numerical bound of 1 located on the right side of (79). When l is sufficiently large to satisfy (73), (77) may then be simplified using [16, # 748, p. 88]. Upon replacing $R_l\,(k)$ by r_{l+1}, we have proven the following

Corollary: For l large enough (80) suffices as an upper bound[19] to the percent error for the admissible class of alternating series. Thus,

$$|\,\delta\eta_l(k)| \le \left|\frac{r_{l+1}}{S_l(k)}\right|\left|1+\left|\frac{r_{l+1}}{S_l(k)}\right|\right|. \tag{80}$$

Lastly, although $\eta(k)$ is explicitly unknown, we can bound its values above and below with the partial sums $S_l(k)$. For l odd it is clear [17, p. 371] that the following is true,

$$S_{l+1}(k) \;\le\; \eta(k) \;\le S_l(k), \text{l odd \& l} \ge 1. \tag{81}$$

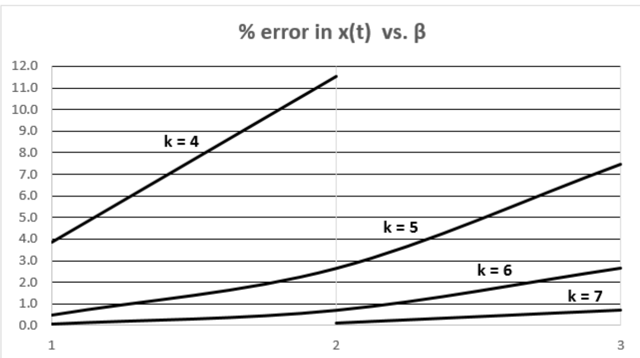

Figure 3. Summary of distortion vs. β & k from equation (60) for TE & LE

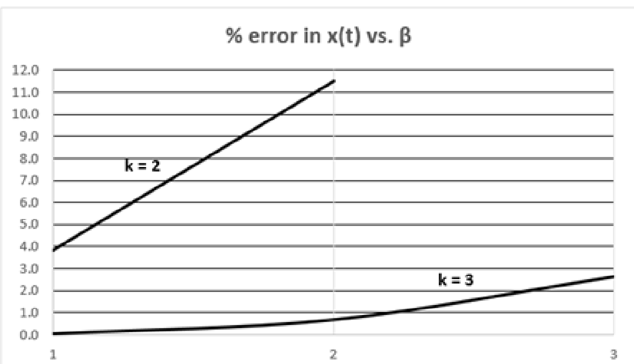

Figure 4. Summary of distortion vs. β & k from equation (70) for DE

This property provides numerical results which complement (77). Equations (71) to (81) will be applied to the Bessel function series coefficients located in Tables 1(a) and 2(a). These tables are structured in the following way; the r^{th} row along any column represents the value of the r^{th} term in (60) excluding the $(-1)^{r-1}$ factor. Each column represents a given choice of the variables β and k. In each column as terms decrease monotonically the value of the term is taken as zero when at least 7 of the first digits are zero. Partial sums $S_l(k)$ and bounds on the error $\delta\eta_l(k)$ for various choices of the integer l are displayed in Tab.'s 1(b) and 2(b) for selected values of k and β.

The information in Tab.'s 1(b) and 2(b) permits us to calculate $\eta(k)$ from its corresponding estimate $S_l(k)$. To do this simply multiply the appropriate $S_l(k)$ by "2" (i.e.; see "2" in footnote 10, (59b)). Further multiplication of $\eta(k)$ by "100" calculates the percent error in the demodulation of x(t). Information gathered in this way was used to construct a design graph for TE and LE PWM in Fig. 3. Fig. 3 displays percent distortion error vs β for various k values. Thus, the engineer may readily choose the smallest sampling rate k consistent with performance requirements for such links. An entirely analogous development applies to equation (70) for DE PWM whose results appear in Fig. 4.

8. Application of the Demodulation Theorem

An application of the demodulation theorem is in order and demonstrates the utility of the results of the previous section.

Application Example: Consider TEPWM and determine the sampling rate k required for β = 2 in order to achieve at most 3% total harmonic distortion. Explore similar design choices for LEPWM and DEPWM.

Solution: For TEPWM the requirements stated in part 1 of the demodulation theorem for (60) allow for an otherwise unrestricted choice of k. The results contained in Fig. 3 suggest that an appropriate choice for k is k = 5. For LEPWM the requirements of part 2 of the theorem require the additional constraint that k be an even number if (60) is to describe the distortion. Again, referring to Fig. 3 we see that k = 6 suffices in order to meet (and in fact exceed) the required distortion level. For DEPWM the requirements of part 3 of the theorem suggest that upon replacing (60) by (70) and referring, now, to Fig. 4 the choice of k = 3 exceeds the requirements and is smaller than the value of k for the TE and the LE cases just considered. So, an added bonus is achieved with DE since *we only require half of the k!* Thus, DE is superior to TE and LE. Physically, DE uses double the number of samples per interval explaining why only half the k is required.

9. Comparison with the Work of Others

Holmes, *et. al.*, [10], use a double Fourier series method to develop a time domain equation (p. 111, eq. 3.26) for the modulated signal which is similar to either (15), (16), or (21)

---

[18] It is clear [15] that $R_l\,(k) \;\to 0$. In general [15] $S_l(k) \;\to\; L$, where L is a finite limit. It should be clear that in the context of this paper L is required to be nonzero for admissibility.

[19] No claim is made as to the optimality or uniqueness of this bound compared to other bounds used herein or elsewhere.

as developed in the present work using the pseudo-static methodology. Distortion is defined differently for their application. Higher k values were required to lessen the effects of distortion as compared to the work described herein. This exhibits a certain consistency with the present work; Holmes work, however, is otherwise very distinct from the present work.

The work summarized in Wilson, *et. al.* [14] provides a more interesting comparison as there is greater overlap in the work. Equation 4.1 in chapter 4.0, [p. 96, 14] is also similar to (15), (16), or (21) in the present. Wilson, *et. al.* use Equation 4.8, [p. 112, 14] is to estimate distortion error. Equation 4.8 [p. 112, 14] is a truncated version of equation 4.1, [p.96, 14]. This is similar in manner to the way the present authors have analyzed the distortion error with the exception that *l* is limited to 1 in [14]. The contrast between the procedure used by Wilson, *et. al.*, [14] and the present authors is that the present authors have the benefit of knowing that (60) is an alternating series with many properties. It seems logical to assume that absent this information, Wilson, *et. al.* would likely do the next best thing which is to engage in experimentation to lend independent validity to their process of truncation. This is illustrated in results displayed in Fig. 4.15 [p. 112,14]. The work of Wilson, *et. al.* and the present work are somewhat complementary in this regard.

10. Conclusions

A proof is provided herein for the Pseudo-Static theorem. This proof is elementary in nature. The Pseudo-Static theorem establishes the exactness of Pseudo-Static spectral analysis, without the need to introduce superfluous constraints. This is physically significant and is in complete agreement with the work of Bennett, *op. cit.*. The distortion is understood for three types of natural PWM and is quantified in terms of a pair of alternating series each of which exhibits the Leibnitz null-monotone property. The benefit of such series is used to great advantage in numerical work, especially when presented in a tabular and graphical form which permits the design engineer to easily understand the distortion in terms of the parameters β and k.

REFERENCES

[1] Starr, A.T., 1952, Radio and Radar Techniques, Pittman and Sons, LTD (London).

[2] Zukui Song, Dilip V. Sarwate, The Frequency Spectrum of pulse width modulated signals, 20003 Elsevier, Signal Processing, vol 83, pgs. 2227-2258.

[3] E.T. Whittaker, G.N. Watson, A course of Modern Analysis, p. 132, 4th edition, Cambridge 1952.

[4] Suh, S.Y., Pulse Width Modulation for Analog Fiber-Optic Communication, Journal 0f Lightwave Technology, Vol. LT. 5, No. 1, January 1987.

[5] Z. Ghassemlooy, B. Wilson, Optical PWM Data Link for High Quality Video and Audio Signals, IEEE Transactions on Consumer Electronics, vol. 40, No. 1, February 1994.

[6] B. Wilson, Z. Ghassemlooy, Pulse time Modulation techniques for optical communications: a review, IEE Proceedings J, Vol. 40 No. 6 December 1993.

[7] W. R Bennett, New Results in the Calculation of modulation components, Bell Syst. Tech, J, 1933, 12,pp. 228-243.

[8] H. S. Black, Modulation Theory, Van Nostrand, New York, 1953, Chapter.

[9] A. Papoulis, Signal Analysis, McGraw-Hill, New York, 1977, pp. 196,197.

[10] D. Grahme Holmes, Thomas A. Lipo, Pulse Width Modulation for Power Converters, IEEE Press, Wiley Interscience, 2003.

[11] G. N. Watson, A Treatise on the Theory of Bessel Functions, Cambridge University Press, Second edition, 1966.

[12] T. J. Bromwich, Theory of Infinite Series, McMillian and Co., Limited, Second Edition, 1949.

[13] E. Jahnke and F. Emde, Tables of functions With Formulae and Curves, Dover Publications, New York, pp. 170-182.

[14] B. Wilson, Z. Ghassemlooy and I. Darwazeh, "Analogue Optical Fibre Communciations", IEE Telecommunications Series 32, 1995.

[15] K. Knopp, "Theory and Application of Infinite Series", Blackie & Son, 1944.

[16] B. O. Peirce, "A Short Table of Integrals", Ginn and Co., 1929.

[17] R. Courant, "Differential and Integral Calculus", Vol I, Interscience, 1937.